Carboxyatractyloside effects on brown-fat mitochondria imply that the adenine nucleotide translocator isoforms ANT1 and ANT2 may be responsible for basal and fatty-acid-induced uncoupling respectively

Irina G. SHABALINA, Tatiana V. KRAMAROVA, Jan NEDERGAARD and Barbara CANNON[1]

The Wenner-Gren Institute, The Arrhenius Laboratories F3, Stockholm University, SE-106 91 Stockholm, Sweden

In brown-fat mitochondria, fatty acids induce thermogenic uncoupling through activation of UCP1 (uncoupling protein 1). However, even in brown-fat mitochondria from UCP1$^{-/-}$ mice, fatty-acid-induced uncoupling exists. In the present investigation, we used the inhibitor CAtr (carboxyatractyloside) to examine the involvement of the ANT (adenine nucleotide translocator) in the mediation of this UCP1-independent fatty-acid-induced uncoupling in brown-fat mitochondria. We found that the contribution of ANT to fatty-acid-induced uncoupling in UCP1$^{-/-}$ brown-fat mitochondria was minimal (whereas it was responsible for nearly half the fatty-acid-induced uncoupling in liver mitochondria). As compared with liver mitochondria, brown-fat mitochondria exhibit a relatively high (UCP1-independent) basal respiration ('proton leak'). Unexpectedly, a large fraction of this high basal respiration was sensitive to CAtr, whereas in liver mitochondria, basal respiration was CAtr-insensitive. Total ANT protein levels were similar in brown-fat mitochondria from wild-type mice and in liver mitochondria, but the level was increased in brown-fat mitochondria from UCP1$^{-/-}$ mice. However, in liver, only Ant2 mRNA was found, whereas in brown adipose tissue, Ant1 and Ant2 mRNA levels were equal. The data are therefore compatible with a tentative model in which the ANT2 isoform mediates fatty-acid-induced uncoupling, whereas the ANT1 isoform may mediate a significant part of the high basal proton leak in brown-fat mitochondria.

Key words: ATP/ADP-carrier isoform, basal proton leak, brown adipose tissue, fatty-acid-induced uncoupling, liver mitochondrion, uncoupling protein 1 (UCP1).

INTRODUCTION

When added to brown-fat mitochondria where the activity of UCP1 (uncoupling protein 1) has been inhibited by purine nucleotides such as GDP, fatty acids (re)activate respiration by overcoming the inhibition of UCP1; this is considered to be the mechanism for stimulation of thermogenesis in BAT (brown adipose tissue) (reviewed in [1–3]). However, not only such coupled brown-fat mitochondria, but also coupled mitochondria from other tissues become uncoupled in response to the addition of fatty acids (reviewed in [4,5]). It has therefore been proposed that, besides UCP1, several other mitochondrial inner membrane anion carrier proteins may mediate fatty-acid-induced uncoupling. The suggested proteins include UCP2, UCP3, the aspartate/glutamate carrier, the dicarboxylate carrier and the phosphate carrier, but particularly, and first suggested, the ANT (adenine nucleotide translocator) (reviewed in [4–6]).

Although such UCP1-independent fatty-acid-induced uncoupling could be suggested to be a non-specific and physiologically irrelevant experimental effect, the possibility of a physiological role has also been discussed. A suggested hypothesis is that fatty-acid-induced ANT-mediated uncoupling could play a role in thermoregulatory heat production in tissues lacking UCP1. Thus ANT-mediated mitochondrial heat production has been proposed to occur in the livers of ground squirrels during hibernation and arousal [7]. Similarly, in several other species and in various tissues, ANT has been suggested to be involved in mitochondrial uncoupling under conditions of cold stress: in rat heart [8], in rodent and bird skeletal muscles [9–12] and even in potato tuber [13].

Brown-fat mitochondria from UCP1-knockout mice also demonstrate fatty-acid-induced uncoupling (although with much lower affinity for fatty acids than UCP1-containing brown-fat mitochondria) [2,14]. The nature of this fatty-acid-induced UCP1-independent uncoupling is presently unknown. We have therefore investigated the involvement of ANT in the mechanism of fatty-acid-induced uncoupling in brown-fat mitochondria from UCP1$^{-/-}$ mice.

EXPERIMENTAL

Animals

UCP1-knockout mice (progeny of those described previously [15]) were backcrossed to C57Bl/6 for ten generations and after intercrossing were maintained as UCP1$^{-/-}$ and UCP1$^{+/+}$ (wild-type) strains. The mice were fed *ad libitum* (R70 Standard Diet; Lactamin), had free access to water, and were kept on a 12 h/12 h light/dark cycle, at a normal (24 °C) animal house temperature. Adult (8–12-week-old) male mice were used for the experiments. The experiments were approved by the Animal Ethics Committee of the North Stockholm Region.

Tissue collection and mitochondrial isolation

Both brown-fat and liver mitochondria were prepared by differential centrifugation principally as described previously [14]. For isolation of mitochondria, ice-cold medium containing 250 mM sucrose and 0.3 % (w/v) fatty-acid-free BSA (plus 20 mM potassium Tes and 1 mM EDTA for liver) was used.

After centrifugation (8500 g for 10 min at 0–2 °C), the resulting mitochondrial pellet was resuspended in the same medium, but albumin-free. The concentration of mitochondrial protein was measured using fluorescamine with BSA as the standard, and the suspensions were diluted to stock concentrations of 25 mg of mitochondrial protein per ml of 125 mM sucrose with 0.2 % fatty-acid-free BSA. With regard to liver mitochondria, most of the data presented are compiled from both wild-type and UCP1$^{-/-}$ mice, based on the data shown in Figure 1. The mitochondrial suspensions were kept on ice and used for no longer than 4 h after isolation.

Oxygen consumption

Mitochondria, at a final concentration of 0.5 mg of mitochondrial protein per ml, were added to 1.1 ml of a continuously stirred incubation medium consisting of 125 mM sucrose, 20 mM Tris/HCl (pH 7.2), 2 mM MgCl$_2$, 1 mM EDTA, 0.1 % fatty-acid-free BSA, 4 mM potassium phosphate and 3 μg/ml oligomycin. The substrate was 5 mM pyruvate plus 3 mM malate; for liver mitochondria, 5 mM glutamate plus 3 mM malate was also used where indicated. Oxygen consumption rates were monitored with a Clark-type oxygen electrode (Yellow Springs Instrument) in a sealed chamber at 37 °C, as described previously [14]. The free concentrations of oleate and palmitate were calculated using the equation described in [16] for the binding of fatty acid to BSA at 37 °C: [free oleate] (nM) $= 6.5n - 0.19 + 0.13\exp(1.54n)$, where n is the molar ratio of oleate to albumin. Concentration–response curve data were analysed with the general fit option of the KaleidaGraph application for Macintosh for adherence to simple Michaelis–Menten kinetics, $V(x) = \text{basal} + \Delta V_{\text{max}} \times [x/(K_{\text{m}} + x)]$, where x is the concentration of oleate.

Mitochondrial swelling

Mitochondrial swelling was monitored as the change in absorbance at 540 nm in an Aminco DW-2 UV-VIS spectrophotometer. The mitochondrial incubation medium and the experimental conditions were as those described for the oxygen consumption experiments. The substrate was 5 mM pyruvate plus 3 mM malate.

Immunoblotting

For immunoblot analysis, aliquots of freshly isolated mitochondrial suspensions were stored at −80 °C after supplementation with protease inhibitor cocktail (Complete™ Mini; Roche). Protein concentrations of the thawed mitochondrial samples were re-quantified using the Lowry method. Mitochondrial samples were separated on SDS/15 % polyacrylamide gels (15 μg/lane) and proteins were electrotransferred on to a PVDF membrane. The membrane was blotted with polyclonal anti-ANT antibodies that detect both ANT1 and ANT2 isoforms (sc-9299; dilution 1:500; Santa Cruz Biotechnology), and secondary antibodies conjugated with HRP (horseradish peroxidase) (anti-goat, dilution 1:2000; Dako). For COX1 (cytochrome c oxidase subunit 1) determination, the membranes used for detection of ANT were blotted, after stripping, with monoclonal anti-COX1 antibodies (Molecular Probes), diluted 1:2000, and secondary antibodies conjugated with HRP (anti-mouse, dilution 1:2000; Cell Signalling Technology). Membranes were incubated in ECL® reagents (Amersham Biosciences) and the chemiluminescence signal was detected with a CCD (charge-coupled-device) camera (Fuji) and quantified using Image Gauge v. 3.45 (FujiFilm) software.

Real-time relative quantitative RT (reverse transcriptase)-PCR

Animals were anaesthetized by a mixture of 79 % CO$_2$ and 21 % O$_2$ and decapitated; tissues were dissected and immediately placed in excess amounts of RNAlater (Qiagen). Total RNA was extracted using Ultraspec (Biotecx) and RNeasy kit (Qiagen) and was on-column treated with RNase-free DNase I (Qiagen) according to the instructions of the manufacturer. RNA integrity was assessed by agarose–formaldehyde gel electrophoresis. Then, 500 ng of total RNA and random decamers (Ambion) were used to synthesize first-strand cDNA by MMLV (Moloney-murine-leukaemia virus) RT (Invitrogen). Real-time quantitative RT-PCR was performed on ABI Prism® 7000 sequence detection system (Applied Biosystems) using SYBR® Green PCR Master Mix (Applied Biosystems), according to the instructions of the manufacturer. PCR was performed with primers for the Ant1 isoform (forward, 5′-AAAAATATGTGTAATACCC-AAGCTCACA-3′; reverse, 5′-TGTTTTCTTTCCTCAAGAATA-GTCTGTTAAAC-3′), the Ant2 isoform (forward, 5′-AGGGCG-CATGGTCCAA-3′; reverse, 5′-ATCTCATCATACAAGACAA-GCACAAAC-3′) and for 18 S ribosomal RNA (forward, 5′-GGG-CCTCGAAAGAGTCCTGTA-3′; reverse, 5′-TACCCACTCCC-GACCCG-3′). The primers (that are specific for the mouse ANT isoforms) were designed with the Primer Express® software (Applied Biosystems). All primer pairs have a 60 °C annealing temperature. PCR premixes that contained 1 × Master Mix, 25 ng of cDNA, 400 ng each of forward and reverse primers in a final volume of 25 μl were prepared and divided into aliquots in duplicate into MicroAmp™ optical 96-well reaction plates. RT-negative controls and non-template controls were included in all experimental runs. Known amounts of cDNA for Ant1, Ant2 and 18 S were used to generate standard curves. For each unknown sample the relative amount was calculated using linear regression analysis from their respective standard curves and normalized to 18 S. Each sample was analysed in two to four separate experiments.

Chemicals

Fatty-acid-free BSA, fraction V, was from Roche Diagnostics. Oleic and palmitic acids (sodium salts), FCCP (carbonyl cyanide p-trifluoromethoxyphenylhydrazone), oligomycin, GDP (sodium salt), L(−)malic acid (disodium salt), pyruvate (sodium salt) and EDTA were all from Sigma. CAtr (carboxyatractyloside) was from Calbiochem-Novobiochem. Fluorescamine {4-phenyl spiro-[furan-2(3H),1-phthalan]-3,3′-dione} was from Fluka Chemie. GDP was dissolved in 20 mM Tes (pH 7.2) and the pH of the solution was readjusted to 7.2. FCCP was dissolved in 95 % ethanol and diluted in 50 % ethanol; oligomycin was dissolved in 95 % ethanol. Oleate (sodium salt) was dissolved in 50 % ethanol, divided into small aliquots, and stored under nitrogen at −20 °C. Ethanol at a final concentration of 0.1 % did not in itself have any effects on the parameters measured.
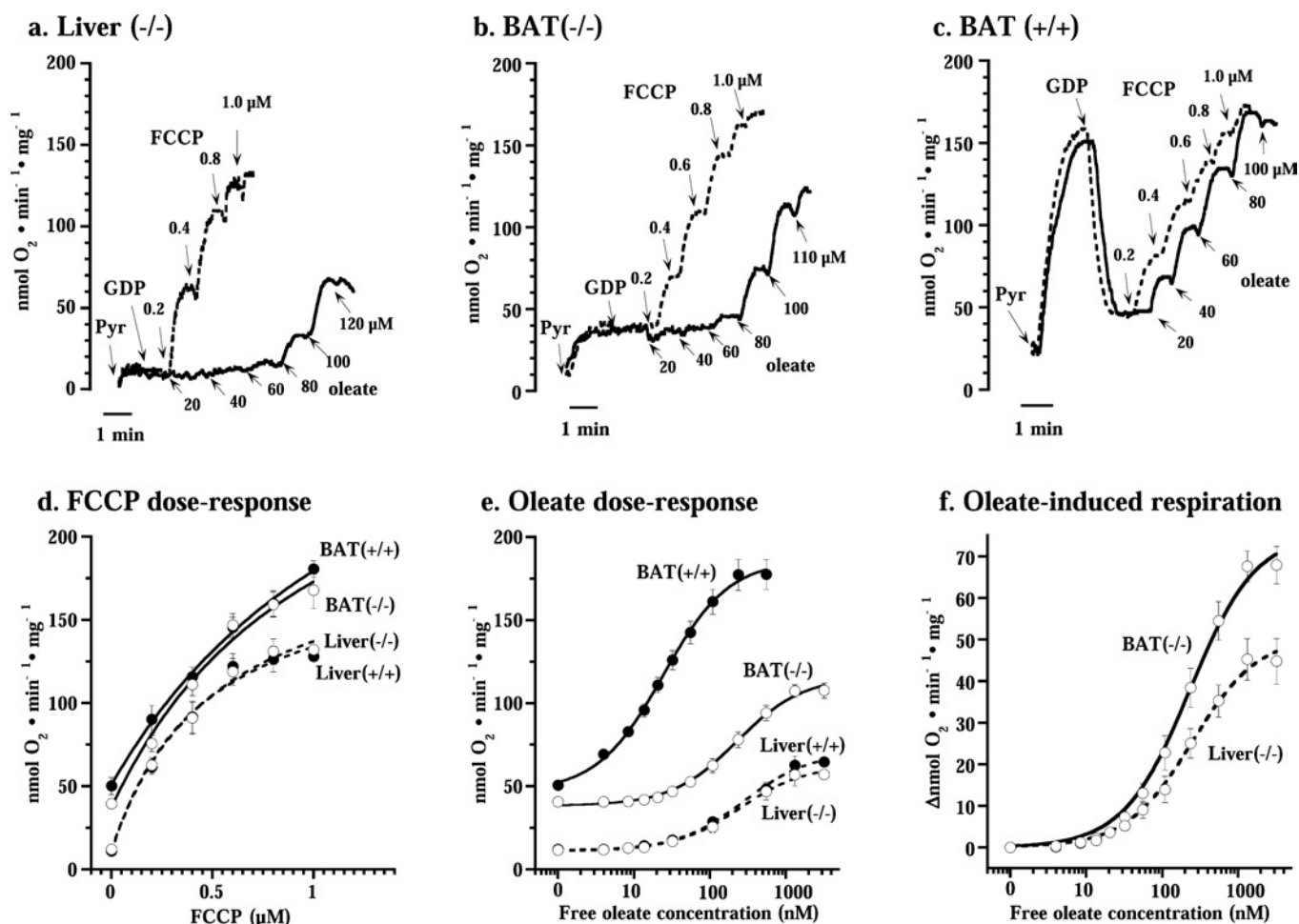
Statistics

All data are expressed as means ± S.E.M. Statistical analysis for the comparison of two groups was performed using Student's t test.

RESULTS

Sensitivity of mitochondria to artificial uncouplers

To examine the nature of fatty-acid-induced UCP1-independent uncoupling in brown-fat mitochondria, we examined

Figure 1   Fatty acid uncoupling efficiency in brown-fat mitochondria and liver from wild-type and UCP1^{−/−} mice

Representative traces showing the effects of oleate (solid line) and FCCP (broken line) on respiration of liver mitohondria from UCP1^{−/−} mice (**a**) and brown-fat mitochondria from UCP1^{−/−} (**b**) and wild-type (**c**) mice. Pyr, addition of 5 mM pyruvate; GDP, addition of 1 mM GDP. FCCP and oleate were successively added to the concentrations indicated. (**d**) Dose–response curve for FCCP compiled from experiments as in (**a**–**c**). Values are means $\pm$ S.E.M. from five to seven independent mitochondrial preparations. Curves were drawn for simple Michaelis–Menten kinetics. (**e** and **f**) Oleate concentration–response curves for brown-fat (solid line) and liver (broken line) mitochondria from wild-type and UCP1^{−/−} mice. The experiments were performed principally as those illustrated in (**a**–**c**). The brown-fat data set in (**d**–**f**) includes a few also included in [14]; however, all brown-fat experiments presented here (but not all in [14]) had been performed in parallel with liver preparations. In (**f**), the change in oxygen consumption (Δ nmol of $O_2 \cdot min^{-1} \cdot mg$ of protein^{-1}) from the coupled state (in the presence of 1 mM GDP) is shown. The points are means $\pm$ S.E.M. for seven to nine independent mitochondrial isolations for each group. The x-axis indicates the free oleate concentrations calculated as described in the Experimental section. Curves were drawn for simple Michaelis–Menten kinetics. For ΔV_{max} and K_m calculations, concentration–response curves were individually analysed in each mitochondrial preparation. These results are shown in Table 1.

mitochondria from BAT of wild-type and UCP1^{−/−} mice. As reference mitochondria we used liver mitochondria, since fatty-acid-induced ANT-mediated uncoupling has been demonstrated in liver mitochondria [7,17,18] and liver mitochondria do not express UCP1 (or UCP2 or UCP3) [19].

To characterize the sensitivity of the different mitochondrial preparations to fatty-acid-induced uncoupling, it was first necessary to examine whether the different types of mitochondria were inherently different in their general uncoupling response. We therefore examined the sensitivity of the different mitochondrial preparations to the uncoupling effect of the chemical uncoupler FCCP. FCCP-induced uncoupling is not expected to be mediated by a specific protein (or by any protein).

Liver mitochondria from either wild-type (results not shown) or UCP1^{−/−} (Figure 1a) mice were well coupled, i.e. exhibited a very low rate of oxygen consumption in the presence of the substrate pyruvate (plus malate). This rate was unaffected by the addition of GDP (necessary in the brown-fat studies) but could be highly stimulated by the artificial uncoupler FCCP (Figure 1a). Brown-

fat mitochondria from UCP1^{−/−} mice displayed a higher rate of basal respiration than liver mitochondria (Figure 1b) but were, as demonstrated previously [14,20], well coupled, in that they responded well to FCCP. Due to the presence of UCP1, brown-fat mitochondria from wild-type mice exhibited a spontaneous very high rate of oxygen consumption (Figure 1c), but this high rate was inhibited by GDP (to exactly the basal level seen in the brown-fat mitochondria from UCP1^{−/−} mice) and the mitochondria were then responsive to FCCP (in agreement with established brown-fat mitochondria characteristics).

Thus the rates of basal respiration (i.e. the rate in the presence of GDP) were significantly higher in brown-fat mitochondria than in liver mitochondria (Figure 1 and Table 1), and these higher rates were independent of the presence of UCP1. The higher levels of basal respiration (higher 'proton leak') in brown-fat mitochondria than in liver mitochondria were thus not due to 'leaky' UCP1 but must be mediated in another way.

All four types of mitochondria exhibited very similar sensitivities to FCCP (Figures 1a–1c). In Figure 1(d), we have compiled

Table 1   Comparison of mitochondrial oxygen consumption from liver and BAT of UCP1$^{-/-}$ and wild-type mice

Concentration–response curve experiments were performed as shown in Figure 1 with pyruvate ($+$ malate) as substrate. The oxygen consumption and maximal oxidative capacity of mitochondria are expressed as nmol of $O_2 \cdot min^{-1} \cdot mg$ of protein^{-1}. ΔFCCP is the increase observed after a maximal dose (1 μM) of FCCP. The K_m (expressed as nM free oleate) and the ΔV_{max} values were obtained from fitting the data to Michaelis–Menten kinetics as shown in Figure 1. The values are means $\pm$ S.E.M. for six to nine independent mitochondrial preparations. **$P < 0.01$ and ***$P < 0.001$, significantly different from UCP1-containing mitochondria (wild-type) BAT. †$P < 0.01$ and ††$P < 0.05$, significant difference between liver and UCP1$^{-/-}$ BAT mitochondria.

Tissue	Mouse strain	Oxygen consumption in the presence of 1 mM GDP	Maximal oxygen consumption stimulated by FCCP, ΔFCCP	K_m for oleate	Maximal oxygen consumption stimulated by oleate, ΔV_{max}
Liver	UCP1$^{-/-}$	11 $+$ 1***†	116 $+$ 7*††	266 $+$ 34***	55 $+$ 6***††
	Wild-type	12 $+$ 1***†	115 $+$ 5*††	279 $+$ 35***	62 $+$ 1***††
BAT	UCP1$^{-/-}$	42 $+$ 4	131 $+$ 8	281 $+$ 36***	82 $+$ 5***
	Wild-type	50 $+$ 4	132 $+$ 7	28 $+$ 4	143 $+$ 10

results from several experiments. The response to FCCP was quantitatively identical whether the mitochondria were isolated from wild-type or UCP1$^{-/-}$ mice, and there was only a small difference in the sensitivity to FCCP between liver and brown-fat mitochondria. The maximal response to FCCP was, however, somewhat higher in brown-fat mitochondria than in liver mitochondria (Figure 1d and Table 1). Thus there was no indication that UCP1 knockout affected the general uncoupling characteristics of the mitochondria.

Sensitivity of mitochondria to fatty-acid-induced uncoupling

We then examined the sensitivity of the four different mitochondrial preparations to fatty acids (here oleate). Oleate was able to stimulate oxygen consumption in all four types of mitochondria (Figures 1a–1c); results from all types of mitochondria are compiled in Figure 1(e).

In Figure 1(e), the liver concentration–response curve demonstrates that there was no difference in fatty acid sensitivity between liver mitochondria from wild-type and UCP1$^{-/-}$ mice, principally as expected. Analysis for simple Michaelis–Menten kinetics yielded a K_m for oleate of approx. 275 nM for both types of liver mitochondria (Table 1).

The response to oleate of brown-fat mitochondria from UCP1$^{-/-}$ mice was similar to that of liver mitochondria, with a very similar K_m (Table 1). Wild-type brown-fat mitochondria, containing UCP1, were, of course, very sensitive to oleate, as demonstrated previously [14], with a K_m 10-fold lower than that observed in mitochondria without UCP1 (Figure 1 and Table 1).

Thus, although loss of the UCP1 protein from brown-fat mitochondria led to a right-hand shift of the oleate dose–response curve, brown-fat mitochondria from UCP1$^{-/-}$ mice remained sensitive to the uncoupling effect of free fatty acids (as shown previously [14,21]) and demonstrated a K_m for oleate that was practically identical with that of liver mitochondria (Figure 1f and Table 1). This implies a similar mechanism for mediation of this fatty-acid-induced uncoupling in UCP1$^{-/-}$ brown-fat mitochondria as in liver mitochondria, but apparently a mechanism with a somewhat higher capacity: the analysis for simple Michaelis–Menten kinetics yielded extrapolated maximal rates of oxygen consumption (ΔV_{max}) induced by oleate that were 30 % higher in brown-fat mitochondria from UCP1$^{-/-}$ mice than in liver mitochondria (Table 1).

Inhibition of ANT by CAtr

In liver mitochondria, a significant fraction of the uncoupling effect of fatty acids is mediated via ANT [7,17,18]. Whether ANT also mediates this effect in brown-fat mitochondria was therefore the aim of this analysis. For this, the effect of the specific inhibitor of ANT, CAtr, was investigated, as performed previously in other tissues [7,17,18,22]. To establish the optimal concentration of CAtr needed for ANT inhibition, the efficiency of CAtr was first examined in its classical role, i.e. for its ability to inhibit oxidative phosphorylation. In liver mitochondria, full inhibition of the oxygen consumption induced by addition of 450 μM ADP was obtained at a concentration of 0.5 μM CAtr (results not shown). For analysis of the involvement of ANT in the fatty-acid-induced uncoupling, a CAtr concentration that was twice as high as this (i.e. 1 μM) was chosen. This concentration thus induced complete inhibition of ANT, but it had no measurable secondary effects (i.e. it did not affect FCCP-stimulated respiration; results not shown).

Involvement of ANT in basal respiration in brown-fat mitochondria

To facilitate analysis of CAtr effects on the composite respiration after fatty acid addition, we initially examined the effect of CAtr on basal respiration. As expected, CAtr did not inhibit basal respiration in liver mitochondria (Figure 2a). This is in accordance with implications from previous experiments [17,18]. The lack of effect of CAtr was independent of whether GDP was present or not (results not shown).

However, very unexpectedly, in brown-fat mitochondria from UCP1$^{-/-}$ mice, a clear effect of CAtr on basal respiration was observed (Figure 2b). This inhibitory effect was also independent of the presence of GDP (results not shown). In wild-type (UCP1-containing) brown-fat mitochondria where UCP1 activity was inhibited by GDP (Figure 2c), CAtr also had an effect. The CAtr effect was also evident in wild-type brown-fat mitochondria when GDP was absent and UCP1 was thus inherently active (Figure 2d).

Thus the CAtr effect on basal respiration observed specifically in brown-fat mitochondria occurred in the absence of added fatty acids or any other respiratory stimulation. As the ATP-synthase inhibitor oligomycin was present, it was not due to inhibition of ATP synthesis from endogenous ADP. Considering the principally unknown nature of basal respiration, the ability to inhibit a significant part of basal respiration with a specific inhibitor (CAtr) is of particular interest, as it implies a specific mediation of a part of the basal respiration in brown-fat mitochondria, i.e. that ANT has this function in brown-fat mitochondria that have high basal respiration (but not in liver mitochondria).

Involvement of ANT in the fatty-acid-induced uncoupling

Despite the unexpected observation of CAtr inhibition of basal respiration in brown-fat mitochondria, the question remained as to whether fatty-acid-induced UCP1-independent uncoupling in brown-fat mitochondria is mediated via ANT.

In our reference system, liver mitochondria, CAtr markedly reduced oleate-stimulated respiration (Figure 3a), in agreement
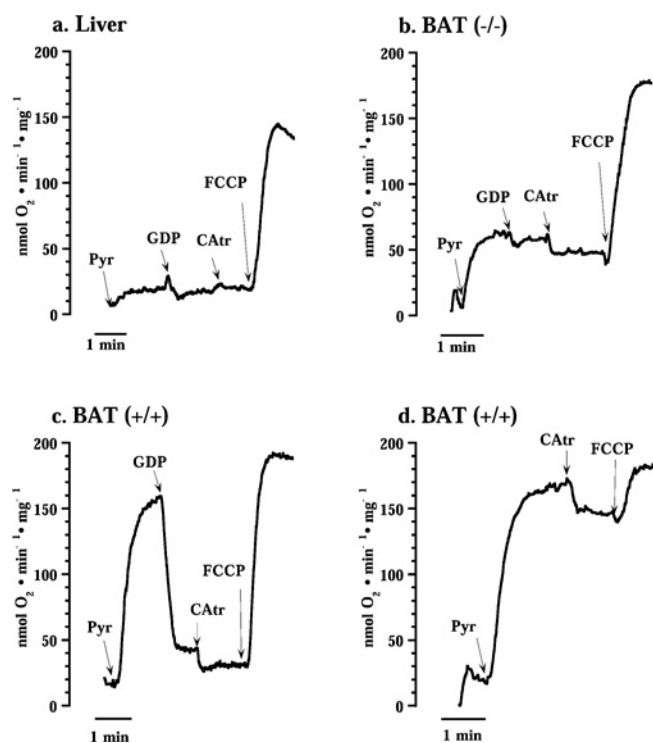
Figure 2   Representative traces showing the effect of CAtr on basal oxygen consumption of liver (a) and brown-fat (b) mitochondria from UCP1⁻/⁻ and mitochondria from wild-type (c and d) mice

Pyr, addition of 5 mM pyruvate; GDP, 1 mM GDP; CAtr, 1.0 μM CAtr; and FCCP, 1.0 μM FCCP.

with a series of previous observations [7,17,18,22]. This effect was observed in liver mitochondria both during respiration with pyruvate plus malate (Figure 3a) or with glutamate plus malate (results not shown). (As brown-fat mitochondria cannot respire on glutamate plus malate, we used pyruvate here also for liver mitochondria to maintain identical experimental conditions.) As CAtr was without effect on basal respiration in liver mitochondria (Figure 2a), the entire decrease in respiration after CAtr addition in Figure 3(a) represented inhibition of fatty-acid-induced uncoupling.

We also examined the CAtr-sensitivity of liver mitochondria when respiration was augmented in a fatty-acid-independent way. This was performed by identifying an amount (0.2 μM) of the

chemical uncoupler FCCP that induced the same increase in respiration as did the oleate amount used above. When this amount of FCCP was added to liver mitochondria, the respiration was thus increased (results not shown), but this increased respiration was fully insensitive to CAtr, in contrast with the oleate-induced respiration. Thus the CAtr effect in liver was not secondary to increased respiration as such, but depended on this respiration being fatty-acid-induced.

In UCP1⁻/⁻ brown-fat mitochondria stimulated by oleate, CAtr had an effect (Figure 3b) apparently similar to that observed in liver mitochondria (Figure 3a). However, the magnitude of this inhibition was of the same magnitude as that seen in the absence of added oleate (Figure 2b) and would thus seem to primarily represent inhibition of basal respiration.

Although all types of mitochondria were treated with the same concentration of oleate, the wild-type brown-fat mitochondria naturally exhibited the highest rate of oleate-induced respiration (Figure 3c). However, also here a CAtr effect was evident. Again, considering the large CAtr effect on basal respiration in wild-type brown-fat mitochondria (Figure 2c), this apparent inhibition of fatty-acid-induced uncoupling was clearly mainly due to the inhibition of basal respiration.

Similar experiments to those shown in Figure 2 were also performed with other fatty acids: palmitate and Medica-16 (β,β'-dimethylhexadecanedioic acid), the latter being an unmetabolizable dicarboxylic fatty acid. The outcome was qualitatively identical (results not shown), indicating that the nature of the fatty acid did not influence the result.

ANT-mediated uncoupling in brown-fat mitochondria is relatively independent of fatty acid concentration

As the response to CAtr appeared similar whether brown-fat mitochondria were first stimulated with fatty acid or not (Figures 3b and 3c compared with Figures 2b–2d), it could not be unequivocally concluded from these experiments whether there actually was a small amount of fatty-acid-induced uncoupling mediated by ANT in brown-fat mitochondria. It was therefore necessary to establish whether the magnitude of the CAtr effect depended on the concentration of fatty acid added. However, fatty acids not only induce mitochondrial uncoupling (increased proton conductance) but may also induce general permeabilization of mitochondria (i.e. non-selective penetration of large molecules leading to mitochondrial swelling) [23,24]. To avoid that this alternative effect of fatty acids interfered with the uncoupling effect under study, mitochondrial swelling experiments were
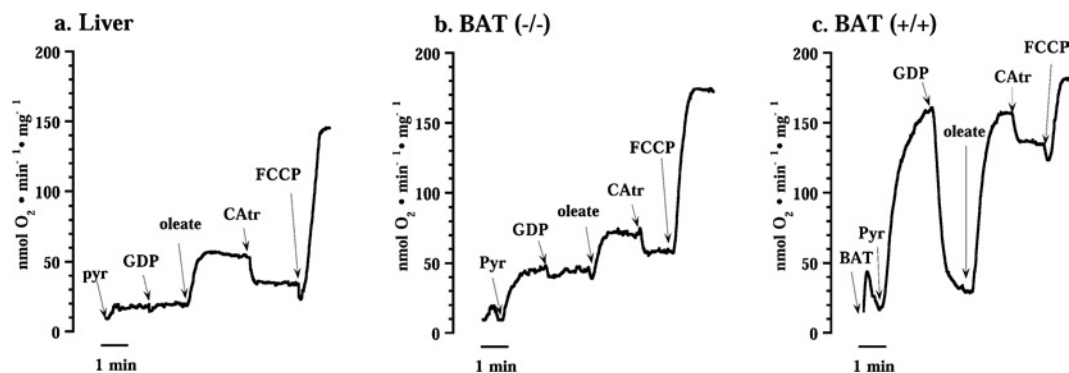
Figure 3   Representative traces showing the effect of CAtr on oleate-stimulated oxygen consumption of liver (a) and brown-fat (b) mitochondria from UCP1⁻/⁻ and mitochondria from wild-type (c) mice

Oleate indicates 70 μM oleate, otherwise additions were the same as in Figure 2.
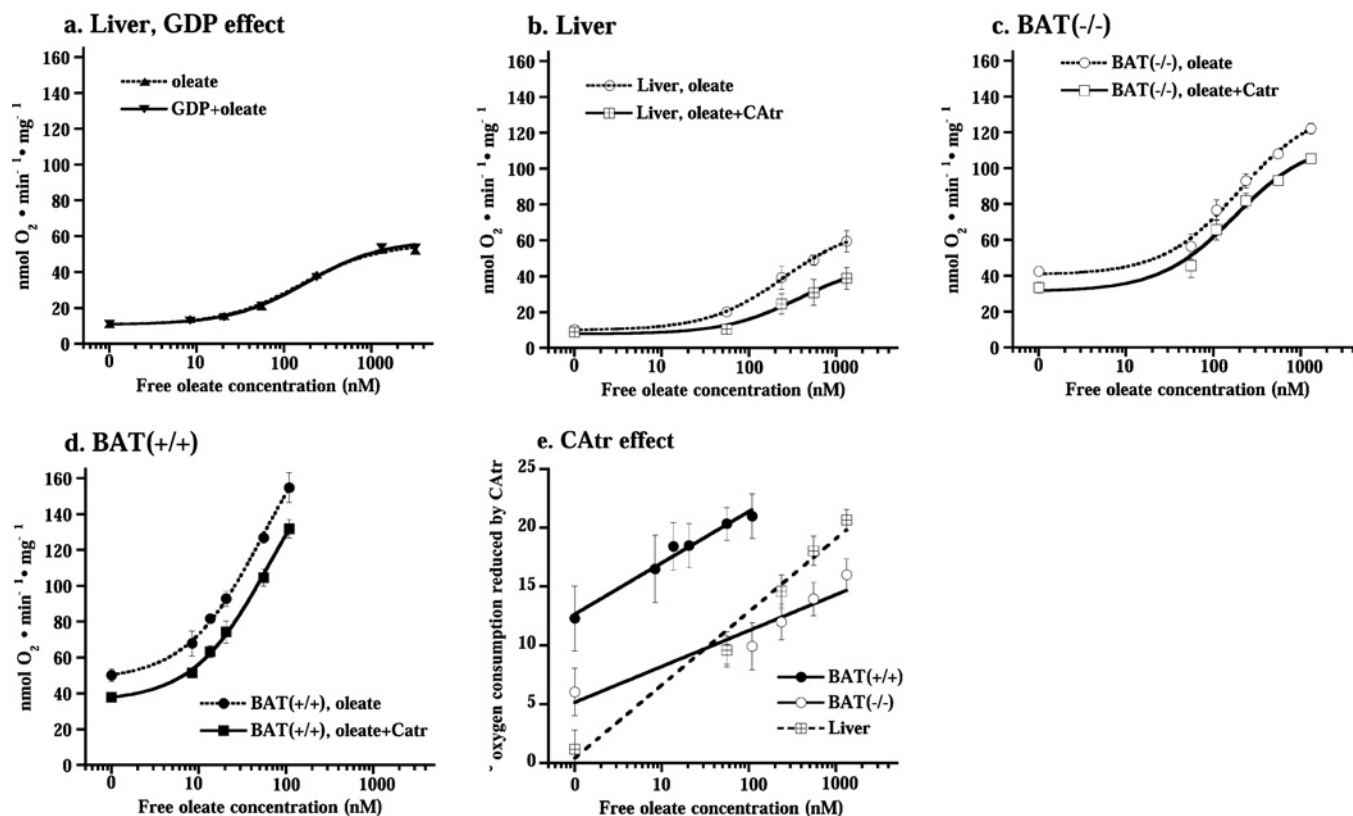
Figure 4   Effect of CAtr on oleate-stimulated oxygen consumption in liver and brown-fat mitochondria

(**a**) Oxygen consumption after successive additions of oleate to liver mitochondria in the presence or absence of 1 mM GDP. (**b–d**) Oxygen consumption after different concentrations of oleate (broken line) or oleate + CAtr (solid line) were added to liver mitochondria (**b**) and brown-fat mitochondria from UCP1$^{-/-}$ (**c**) and wild-type (**d**) mice. The experiments were performed principally as those illustrated in Figure 3, except that in each experiment a different concentration of oleate was added (from 0 to maximally 100 μM). The values represent the means $\pm$ S.E.M. of five independent liver, eight wild-type and eight UCP1$^{-/-}$ brown-fat mitochondrial preparations. (**e**) CAtr effect on oleate-stimulated oxygen consumption. CAtr-reduced oxygen consumption was estimated as basal (in the presence of GDP) respiration or oleate-stimulated respiration minus CAtr-insensitive oxygen consumption (as performed in Figure 3) in the same mitochondrial preparation.

performed, principally as described previously [14,25]. Different oleate concentrations were assessed for their ability to induce mitochondrial swelling. With up to 100 μM added oleate, no swelling was observed (for up to 7 min) in any type of mitochondria investigated, but in all types of mitochondria 120 μM oleate induced a swelling that developed with time (results not shown). Therefore only oleate concentrations up to 100 μM were added in the experiments shown in Figure 4.

We first examined whether the presence of GDP, necessary for experiments with wild-type brown-fat mitochondria, influenced the fatty-acid-sensitivity of liver mitochondria. As seen in Figure 4(a), this was not the case.

The significance of ANT for fatty-acid-induced uncoupling was quantified by experiments principally as those shown in Figure 3 but with different amounts of added oleate. The data are compiled in Figures 4(b)–4(d), where the circles (upper curves) indicate the rates observed directly after oleate addition (compare with Figure 3), whereas the squares (lower curves) indicate the rate observed in the same trace after the further addition of CAtr (compare with Figure 3). The difference between these curves thus constitutes the CAtr effect (i.e. the ANT-mediated uncoupling) and this effect is compiled in Figure 4(e).

In liver mitochondria, there was (in accordance with Figure 2a) no effect of CAtr on basal respiration. An effect became apparent with increasing fatty acid concentrations (Figure 4b), in agreement with [18,22]. As seen, approx. 50 % of the total response to fatty acid was mediated by ANT in these mitochondria. When the

CAtr-sensitive increase in respiration was plotted as a function of fatty acid concentration, the line extrapolated to 0, confirming the absence of effect of CAtr on basal respiration (Figure 4e).

In both types of brown-fat mitochondria, the CAtr effect was very different. The CAtr effect was clearly evident on basal respiration and was only marginally increased with increasing fatty acid concentration (Figures 4c and 4d). Nonetheless, in Figure 4(e), it can be seen that even in these mitochondria there was a component of the fatty-acid-induced uncoupling that could be inhibited by CAtr. However, this component amounted to only approx. 10 % of the total response to fatty acid. Additionally, the curve for the effect of CAtr as a function of fatty acid concentration added did not extrapolate to 0 (Figure 4e). Thus, in brown-fat mitochondria, the CAtr effect was largely independent of fatty acid addition and, conversely, the fatty acid effect was largely independent of ANT activity.

The (small) fraction of fatty-acid-induced uncoupling that could be ascribed to ANT stimulation was approximately the same in brown-fat mitochondria from wild-type or UCP1$^{-/-}$ mice (Figure 4e) and the slope was not significantly different (but was less than half that of liver mitochondria). The fatty-acid-independent ANT-mediated uncoupling was approx. twice as high in wild-type compared with UCP1$^{-/-}$ mitochondria (Figure 4e). It would thus seem that in brown-fat mitochondria the total CAtr response consists of two components: one that is fatty-acid-induced and thus liver-like (but smaller than in liver), and one that is fatty-acid-independent, the magnitude of which is different
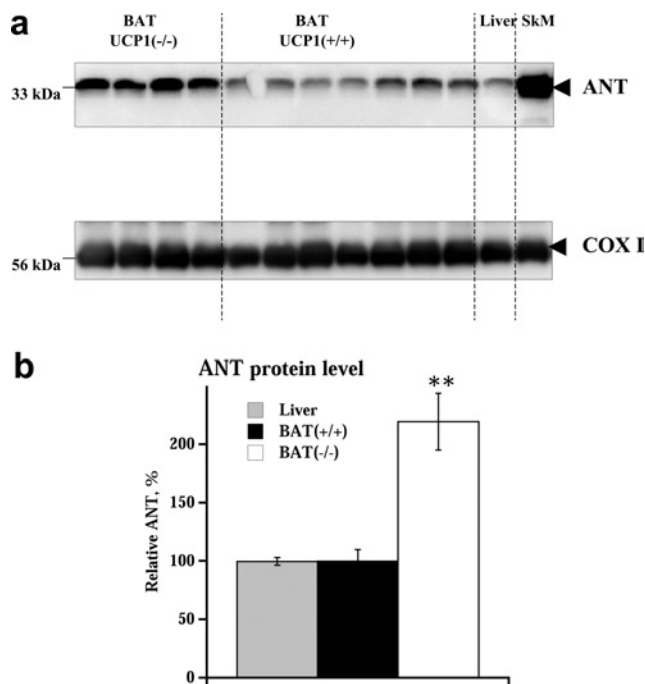
Figure 5   ANT protein levels in brown-fat and liver mitochondria isolated from UCP1$^{-/-}$ and wild-type mice

(**a**) Representative Western-blot analysis of mitochondria (15 μg of mitochondrial protein/lane) isolated from BAT from wild-type and UCP1$^{-/-}$ mice and from liver and skeletal muscle (SkM) from wild-type mice. Upper panel: ANT. Lower panel: COX1. (**b**) Quantification of ANT protein in mitochondria. The level of ANT protein was normalized to COX1 protein level and this ratio was set to 100 % in wild-type brown-fat mitochondria. The values are the means $\pm$ S.E.M. for independent mitochondrial preparations each analysed in duplicate ($n = 7$ for wild-type brown-fat mitochondria, $n = 4$ for UCP1$^{-/-}$ brown-fat mitochondria and $n = 2$ for liver mitochondria). **Significantly different ($P < 0.01$) from UCP1-containing mitochondria (BAT$^{+/+}$).

between brown-fat mitochondria from wild-type and UCP1$^{-/-}$ mice.

CAtr-mediated fatty acid uncoupling in brown-fat mitochondria does not correlate with total ANT protein content

A quantitative dependence of ANT-mediated fatty-acid-induced uncoupling on the content of ANT in mitochondria has been suggested [10,11,18]; however, no information is available concerning the level of ANT protein in BAT.

Oxidative phosphorylation activity is very low in brown-fat mitochondria [20,26,27]; for the mitochondria used in the present study, the ADP-stimulated respiration (defined as the maximal rate of mitochondrial oxygen consumption after addition of ADP minus the rate of oligomycin-insensitive respiration) was 97 ± 9 for liver but only 23 ± 6 and 17 ± 2 nmol of $O_2 \cdot min^{-1} \cdot mg$ of protein^{-1} for UCP1$^{-/-}$ and wild-type brown-fat mitochondria respectively ($n = 7$, 4 and 4 respectively). (The low phosphorylation activity in brown-fat mitochondria can be explained by their low F_o–F_1 ATP synthase content [26,27].) There would therefore be comparatively little need for ANT activity in brown-fat mitochondria compared with liver, and the ANT content would accordingly be expected to be low.

The presence and amount of ANT protein was analysed by immunoblotting (with an antibody that recognizes both ANT isoforms, see below). Unexpectedly, the ANT content was quite high in brown-fat mitochondria, with levels similar to those in liver (Figure 5), and the ANT content was even twice as high in
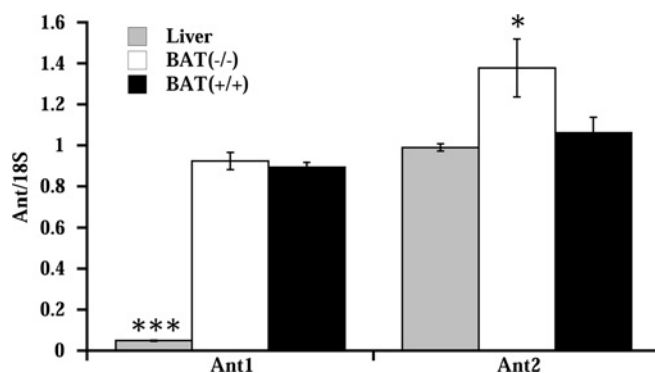
Figure 6   Real-time relative quantitative RT-PCR analysis of transcripts of ANT isoforms in BAT and liver

mRNA levels of the Ant1 and Ant2 isoforms were analysed in liver and in BAT of wild-type (BAT$^{+/+}$) and UCP1$^{-/-}$ (BAT$^{-/-}$) mice relative to 18 S rRNA levels. The values are the means $\pm$ S.E.M. for independent cDNA preparations analysed in duplicate ($n = 4$ for BAT samples and $n = 2$ for liver samples), *$P < 0.05$ and ***$P < 0.001$, significantly different from BAT of wild-type mice (BAT$^{+/+}$)

UCP1$^{-/-}$ brown-fat mitochondria compared with wild-type (and liver) mitochondria (Figure 5).

When this information on ANT protein levels was compared with the bioenergetic data obtained above, it was evident that there was no simple correlation. As the total ANT levels in liver and wild-type brown-fat mitochondria are identical (Figure 5b), it would be expected that the ANT-mediated fatty-acid-induced uncoupling would also be similar; however, it was less than half (Figure 4e).

Ant1 and Ant 2 isoform expression in BAT

ANT exists in several isoforms. Two isoforms, Ant1 and Ant2, are found in mice. The isoforms are differentially distributed in various tissues [28,29]. To investigate which isoforms are found in BAT of mice, we measured Ant1 and Ant2 mRNA levels by real-time quantitative RT-PCR.

In liver only the Ant2 isoform was present (Figure 6), in agreement with results published previously results [29]. In BAT, both Ant isoforms were expressed, at approximately similar levels. In UCP1$^{-/-}$ mice, Ant2 mRNA levels were increased compared with wild-type mice. This increase could contribute to the observed increase in total ANT protein found in UCP1$^{-/-}$ mice (Figure 5).

Based on this difference in Ant isoform pattern between liver and brown-fat mitochondria, it may be possible to suggest that the qualitative differences in CAtr response between the tissues may be explainable by isoform-specific differential properties of the two isoforms. No ANT isoform-specific antibodies are commercially available, and direct evidence of ANT isoform protein levels in the different tissues can therefore not be obtained. However, if Ant1 is the only isoform that mediates CAtr-sensitive (fatty-acid-independent) 'basal' uncoupling, this phenomenon would only be observed in brown-fat mitochondria and not in liver mitochondria. Furthermore, provided that the two mRNAs in BAT are translated at approximately equal efficiencies, the relative content of Ant2 would be lower in brown-fat mitochondria than in liver. If Ant2 is the only isoform that mediates CAtr-sensitive fatty-acid-induced uncoupling, this would explain why this component is relatively lower in brown-fat mitochondria than in liver mitochondria.

DISCUSSION

ANT is generally accepted as being the main mediator of the uncoupling effect of fatty acids in liver and muscle mitochondria. In the present investigation, we examined the involvement of ANT in the mediation of UCP1-independent fatty-acid-induced uncoupling in brown-fat mitochondria. We observed quantitatively that the contribution of ANT to fatty-acid-induced uncoupling in these mitochondria was minimal, but also the qualitatively novel observation that in brown-fat mitochondria a significant fraction of the basal respiration was sensitive to the ANT inhibitor CAtr. The distribution of ANT isoforms was different in liver and BAT: in liver, only Ant2 mRNA was found, whereas in BAT Ant1 and Ant2 were expressed at similar levels. The data are compatible with a model in which the ANT2 isoform is the one that mediates the ANT-dependent fraction of the fatty-acid-induced uncoupling in both liver and brown-fat mitochondria, whereas the ANT1 isoform is the one that mediates the ANT-dependent fraction of the high UCP1-independent basal proton leak in brown-fat mitochondria.

Fatty-acid-induced uncoupling in brown-fat mitochondria is virtually not mediated by ANT

Despite the fact that the fatty-acid-induced uncoupling in brown-fat mitochondria from UCP1$^{-/-}$ mice is higher than that in liver mitochondria (Figure 1), the ANT-mediated part is much smaller, both in relative and absolute terms (Figure 4e): approx. 50 % of the uncoupling effect of fatty acids in liver mitochondria is mediated by ANT, but only approx. 10 % of this uncoupling was mediated by ANT in UCP1$^{-/-}$ brown-fat mitochondria (Figure 4). The question therefore arises as to how the UCP1-independent fatty-acid-induced uncoupling is mediated in brown-fat mitochondria. Membrane carriers other than ANT have been suggested as mediators of fatty-acid-induced uncoupling in different tissues (reviewed in [4–6]). However, these carriers appear even less appropriate than ANT for a role in fatty-acid-induced uncoupling in brown-fat mitochondria. The activity of most mitochondrial carriers is low in brown-fat mitochondria compared with liver mitochondria [30], and for example, the expression of the dicarboxylate carrier is very low [31]. UCP2 protein is not found in the tissue [19], and UCP3 expression is down-regulated in UCP1$^{-/-}$ BAT [32]. Thus it would appear that brown-fat mitochondria possess a high amount of a so far unidentified membrane protein that can mediate fatty-acid-induced uncoupling with a similar affinity to fatty acids as has ANT2.

The ANT-mediated fatty-acid-induced uncoupling component in the UCP1$^{-/-}$ mitochondria was not higher than in the UCP1-containing (wild-type) brown-fat mitochondria (Figure 4e). There is thus no evidence that, in the absence of the normal UCP1-dependent thermogenic process, fatty-acid-induced ANT-mediated uncoupling is increased as a compensatory process, i.e. this process has no thermogenic potential in brown-fat mitochondria, despite the increase in total ANT protein.

Increased ANT content in brown-fat mitochondria from UCP1$^{-/-}$ mice

The increased level of ANT protein in brown-fat mitochondria from UCP1$^{-/-}$ mice compared with wild-type mice (Figure 5) is presumably due to the higher Ant2 mRNA level observed in the BAT of these mice (although there may also be changes in translational efficiency) (Figure 6). The mediation and the functional significance of this increase needs to be discussed. The control of gene expression of the Ant2 isoform has not been extensively

studied, but in the heart it may be under positive thyroid hormone control [33]. We find it likely that in BAT the expression of Ant2 is under adrenergic control, as is mitochondriogenesis in this tissue in general [34]. Ant2 (and Ant1) gene expression is much reduced in the BAT of lactating rats [35], a situation probably associated with a decreased adrenergic stimulation of the tissue [3]. Correspondingly, the increased Ant2 gene expression observed in the present study in the UCP1$^{-/-}$ mouse could result from an increased adrenergic stimulation of the tissue. The expression of several adrenergically controlled genes is increased in the BAT of UCP1$^{-/-}$ mice [36,37]. This probably results from sympathetic hyperactivity (V. Golozoubova, A. Rodriguez, A. Palou, B. Cannon and J. Nedergaard, unpublished work), resulting from a physiological feedback system, attempting to activate the thermogenically non-functional tissue, as suggested previously [38]. The increase in ANT observed in the BAT of UCP1$^{-/-}$ mice is thus probably without functional significance.

A large proportion of basal proton conductance in brown-fat mitochondria depends on ANT

Irrespective of whether they contained UCP1 or not, brown-fat mitochondria had a much higher basal respiratory rate than liver mitochondria (Figures 1a–1c) (basal rate is defined here as that in the presence of GDP to inhibit UCP1). This coincides with the basal rate of brown-fat mitochondria being partly inhibited by CAtr, whereas that of liver mitochondria is unaffected by CAtr (Figures 2 and 4). The effect of CAtr in wild-type mitochondria is not due to CAtr binding to UCP1 [39,40]. Our observations thus imply that a significant fraction of basal respiration, i.e. of the basal proton leak, in isolated brown-fat mitochondria is mediated by ANT.

Despite many suggestions, the nature of the general mitochondrial proton leak is still not understood [41]. Although, for example, phospholipid characteristics have been discussed previously in this content, attention has now turned to the role of specific proteins (e.g. [42]). Recently, ANT was shown to be a significant mediator of the basal proton leak in mitochondria from skeletal muscle and *Drosophila* [43]. Our results would in general support such an additional function of ANT.

A suggestion for the differential uncoupling effects of ANT1 and ANT2 isoforms

In mice, the ANT exists in two isoforms (Ant1 and Ant2), encoded by two separate genes [29]. Ant1 is highly expressed only in heart and skeletal muscle and is nearly absent from liver. Ant2 is ubiquitously expressed but is low in skeletal muscle [28,29]. We found that both isoforms were expressed in BAT at similar levels. Although Ant1 and Ant2 share almost 90 % nucleotide sequence identity, they have been differentially implicated in several cellular functions [44–48]. ANT1 and ANT2 also have a differential distribution in the mitochondrial inner membrane, with ANT1 being found preferentially in the peripheral inner membrane, mainly located in contact sites between the outer and inner mitochondrial membranes, whereas ANT2 is also found in the cristae [45]. To these differential characteristics, we now add the possibility that, at least in BAT, the isoforms are differentially involved in uncoupling functions: ANT1 in 'basal' uncoupling and ANT2 in fatty-acid-induced uncoupling. The suggestion that it is ANT1 that is primarily involved in basal uncoupling (proton leak) is in accordance with the fact that Brand et al. [43] investigated transgenic mice with a specific knockout of ANT1, arriving at the general conclusion that ANT is involved in mediating basal proton leak. Based on the present results, we

would suggest that this function is restricted to ANT1. Conversely, we would suggest that fatty-acid-induced uncoupling is restricted to the ANT2 isoform.

Generality of the differential functions of the ANT isoforms

Whether the functional isoform specialization suggested in the present study is relevant for ANT in all tissues cannot be concluded from the current data. The implication would be that, in all tissues where Ant1 is expressed, some of the basal respiration would be sensitive to CAtr. We have confirmed that in skeletal muscle it is the Ant1 isoform that is mainly expressed (results not shown) and that the total amount of ANT protein in muscle is high (Figure 5). The prediction from the above hypothesis is thus that, also in muscle mitochondria, CAtr should be able to inhibit some of the basal proton leak. This has never been directly stated, but re-examination of the literature indicates this to be the case: there is a clear CAtr effect on the basal proton leak mediated by ANT isolated from bovine heart and reconstituted into liposomes [49], and, in muscle mitochondria, effects of CAtr could be observed even in the presence of albumin that should bind all fatty acids [8,12,50]. These observations, although clear from the data presented, were not directly highlighted by the original authors and have therefore been ignored. We have observed that, in skeletal-muscle mitochondria respiring on succinate, a marked $\geqslant 10\%$ inhibition of basal respiration upon addition of CAtr is obtained (results not shown), in accordance with the hypothesis suggested in the present study. The amount of ANT2 in muscle mitochondria (as implied from the Ant1/Ant2 mRNA ratios and from [43]) is probably sufficient to account for the mediation by this isoform of fatty-acid-induced uncoupling in this type of mitochondria, as well as in liver and brown-fat mitochondria.

Thus, although full quantitative association between the amount of ANT and uncoupling does not seem to exist, the data available tend to support a functional difference between the ANT isoforms with respect to basal proton leak (ANT1) and fatty-acid-induced uncoupling (ANT2).

REFERENCES

1 Nicholls, D. G. and Locke, R. M. (1984) Thermogenic mechanisms in brown fat. Physiol. Rev. **64**, 1–64

2 Nedergaard, J., Golozoubova, V., Matthias, A., Asadi, A., Jacobsson, A. and Cannon, B. (2001) UCP1: the only protein able to mediate adaptive non-shivering thermogenesis and metabolic inefficiency. Biochim. Biophys. Acta **1504**, 82–106

3 Cannon, B. and Nedergaard, J. (2004) Brown adipose tissue: function and physiological significance. Physiol. Rev. **84**, 277–359

4 Skulachev, V. P. (1998) Uncoupling: new approaches to an old problem of bioenergetics. Biochim. Biophys. Acta **1363**, 100–124

5 Wojtczak, L., Wieckowski, M. R. and Schönfeld, P. (1998) Protonophoric activity of fatty acid analogs and derivatives in the inner mitochondrial membrane: a further argument for the fatty acid cycling model. Arch. Biochem. Biophys. **357**, 76–84

6 Sluse, F. E., Jarmuszkiewicz, W., Navet, R., Douette, P., Mahy, G. and Sluse-Goffart, C. M. (2006) Mitochondrial UCPs: new insights into regulation and impact. Biochim. Biophys. Acta **1757**, 480–485

7 Brustovetsky, N. N., Amerkanov, Z. G., Yegorova, M. E., Mokhova, E. N. and Skulachev, V. P. (1990) Carboxyatractylate-sensitive uncoupling in liver mitochondria from ground squirrels during hibernation and arousal. FEBS Lett. **272**, 190–192

8 Simonyan, R. A. and Skulachev, V. P. (1998) Thermoregulatory uncoupling in heart muscle mitochondria: involvement of the ATP/ADP antiporter and uncoupling protein. FEBS Lett. **436**, 81–84

9 Simonyan, R. A., Jimenez, M., Ceddia, R. B., Giacobino, J. P., Muzzin, P. and Skulachev, V. P. (2001) Cold-induced changes in the energy coupling and the UCP3 level in rodent skeletal muscles. Biochim. Biophys. Acta **1505**, 271–279

10 Toyomizu, M., Ueda, M., Sato, S., Seki, Y., Sato, K. and Akiba, Y. (2002) Cold-induced mitochondrial uncoupling and expression of chicken UCP and ANT mRNA in chicken skeletal muscle. FEBS Lett. **529**, 313–318

11 Talbot, D. A., Duchamp, C., Rey, B., Hanuise, N., Rouanet, J. L., Sibille, B. and Brand, M. D. (2004) Uncoupling protein and ATP/ADP carrier increase mitochondrial proton conductance after cold adaptation of king penguins. J. Physiol. **558**, 123–135

12 Schaefer, C. D. and Staples, J. F. (2006) Mitochondrial metabolism in mammalian cold-acclimation: magnitude and mechanisms of fatty acid uncoupling. J. Therm. Biol. **31**, 355–361

13 Popov, V. N., Markova, O. V., Mokhova, E. N. and Skulachev, V. P. (2002) Effects of cold exposure *in vivo* and uncouplers and recouplers *in vitro* on potato tuber mitochondria. Biochim. Biophys. Acta **1553**, 232–237

14 Shabalina, I. G., Jacobsson, A., Cannon, B. and Nedergaard, J. (2004) Native UCP1 displays simple competitive kinetics between the regulators purine nucleotides and fatty acids. J. Biol. Chem. **279**, 38236–38248

15 Enerbäck, S., Jacobsson, A., Simpson, E. M., Guerra, C., Yamashita, H., Harper, M.-E. and Kozak, L. P. (1997) Mice lacking mitochondrial uncoupling protein are cold-sensitive but not obese. Nature **387**, 90–94

16 Richieri, G. V., Anel, A. and Kleinfeld, A. M. (1993) Interactions of long-chain fatty acids and albumin: determination of free fatty acid levels using the fluorescent probe ADIFAB. Biochemistry **32**, 7574–7580

17 Brustovetsky, N. N., Dedukhova, V. I., Egorova, M. V., Mokhova, E. N. and Skulachev, V. P. (1990) Inhibitors of the ATP/ADP antiporter suppress stimulation of mitochondrial respiration and H+ permeability by palmitate and anionic detergents. FEBS Lett. **272**, 187–189

18 Schönfeld, P. (1990) Does the function of adenine nucleotide translocase in fatty acid uncoupling depend on the type of mitochondria? FEBS Lett. **264**, 246–248

19 Pecqueur, C., Alves-Guerra, M. C., Gelly, C., Levi-Meyrueis, C., Couplan, E., Collins, S., Ricquier, D., Bouillaud, F. and Miroux, B. (2000) Uncoupling protein 2: *in vivo* distribution, induction upon oxidative stress and evidence for translational regulation. J. Biol. Chem. **276**, 8705–8712

20 Matthias, A., Jacobsson, A., Cannon, B. and Nedergaard, J. (1999) The bioenergetics of brown fat mitochondria from UCP1-ablated mice. UCP1 is not involved in fatty acid-induced de-energization. J. Biol. Chem. **274**, 28150–28160

21 Hofmann, W. E., Liu, X., Bearden, C. M., Harper, M. E. and Kozak, L. P. (2001) Effects of genetic background on thermoregulation and fatty acid-induced uncoupling of mitochondria in UCP1-deficient mice. J. Biol. Chem. **276**, 12460–12465

22 Andreyev, A. Y., Bondareva, T. O., Dedukhova, V. I., Mokhova, E. N., Skulachev, V. P., Tsofina, L. M., Volkov, N. I. and Vygodina, T. V. (1989) The ATP/ADP-antiporter is involved in the uncoupling effect of fatty acids on mitochondria. Eur. J. Biochem. **182**, 585–592

23 Wojtczak, L. and Wieckowski, M. R. (1999) The mechanisms of fatty acid-induced proton permeability of the inner mitochondrial membrane. J. Bioenerg. Biomembr. **31**, 447–455

24 Sultan, A. and Sokolove, P. M. (2001) Free fatty acid effects on mitochondrial permeability: an overview. Arch. Biochem. Biophys. **386**, 52–61

25 Silva, J. P., Shabalina, I. G., Dufour, E., Petrovic, N., Backlund, E. C., Hultenby, K., Wibom, R., Nedergaard, J., Cannon, B. and Larsson, N.-G. (2005) SOD2 overexpression: enhanced mitochondrial tolerance but absence of effect on UCP activity. EMBO J. **24**, 4061–4070

26 Cannon, B. and Vogel, G. (1977) The mitochondrial ATPase of brown adipose tissue: purification and comparison with the mitochondrial ATPase from beef heart. FEBS Lett. **76**, 284–289

27 Houstek, J. and Drahota, Z. (1977) Purification and properties of mitochondrial adenosine triphosphatase of hamster brown adipose tissue. Biochim. Biophys. Acta **484**, 127–139

28 Stepien, G., Torroni, A., Chung, A. B., Hodge, J. A. and Wallace, D. C. (1992) Differential expression of adenine nucleotide translocator isoforms in mammalian tissues and during muscle cell differentiation. J. Biol. Chem. **267**, 14592–14597

29 Levy, S. E., Chen, Y. S., Graham, B. H. and Wallace, D. C. (2000) Expression and sequence analysis of the mouse adenine nucleotide translocase 1 and 2 genes. Gene **254**, 57–66

30 Cannon, B., Bernson, V. M. S. and Nedergaard, J. (1984) Metabolic consequences of limited substrate anion permeability in brown fat mitochondria from a hibernator, the golden hamster. Biochim. Biophys. Acta **766**, 483–491

31 Unami, A., Shinohara, Y., Kajimoto, K. and Baba, Y. (2004) Comparison of gene expression profiles between white and brown adipose tissues of rat by microarray analysis. Biochem. Pharmacol. **67**, 555–564

32   Matthias, A., Ohlson, K. E. B., Fredriksson, J. M., Jacobsson, A., Nedergaard, J. and Cannon, B. (2000) Thermogenic responses in brown-fat cells are fully UCP1-dependent: UCP2 or UCP3 do not substitute for UCP1 in adrenergically or fatty acid induced thermogenesis. J. Biol. Chem. **275**, 25073–25081

33   Dummler, K., Muller, S. and Seitz, H. J. (1996) Regulation of adenine nucleotide translocase and glycerol 3-phosphate dehydrogenase expression by thyroid hormones in different rat tissues. Biochem. J. **317**, 913–918

34   Néchad, M., Nedergaard, J. and Cannon, B. (1987) Noradrenergic stimulation of mitochondriogenesis in brown adipocytes differentiating in culture. Am. J. Physiol. **253**, C889–C894

35   Martin, I., Giralt, M., Vinas, O., Iglesias, R., Mampel, T. and Villarroya, F. (1995) Co-ordinate decrease in the expression of the mitochondrial genome and nuclear genes for mitochondrial proteins in the lactation-induced mitochondrial hypotrophy of rat brown fat. Biochem. J. **308**, 749–752

36   Fredriksson, J. M., Nikami, H. and Nedergaard, J. (2005) Cold-induced expression of the VEGF gene in brown adipose tissue is independent of thermogenic oxygen consumption. FEBS Lett. **579**, 5680–5684

37   Nikami, H., Nedergaard, J. and Fredriksson, J. M. (2005) Norepinephrine but not hypoxia stimulates HIF-1α gene expression in brown adipocytes. Biochem. Biophys. Res. Commun. **337**, 121–126

38   Cannon, B., Matthias, A., Golozoubova, V., Ohlson, K. B. E., Andersson, U., Jacobsson, A. and Nedergaard, J. (1999) Unifying and distinguishing features of brown and white adipose tissues: UCP1 versus other UCPs. Prog. Obes. Res. **8**, 13–26

39   Heaton, G. M., Wagenvoord, R. J., Kemp, J. A. and Nicholls, D. G. (1978) Brown-adipose-tissue mitochondria: photoaffinity labelling of the regulatory site of energy dissipation. Eur. J. Biochem. **82**, 515–521

40   Woldegiorgis, G., Duff, T., Contreras, L., Shrago, E. and Ruoho, A. E. (1989) Photoaffinity labeling of hamster brown adipose tissue mitochondria by an [^{125}I] coenzyme A derivative: differential interaction with the uncoupling protein and ADP/ATP carrier. Biochem. Biophys. Res. Commun. **161**, 502–507

41   Brand, M. D., Chien, L. F., Ainscow, E. K., Rolfe, D. F. and Porter, R. K. (1994) The causes and functions of mitochondrial proton leak. Biochim. Biophys. Acta **1187**, 132–139

42   Porter, R. K. (2001) Mitochondrial proton leak: a role for uncoupling proteins 2 and 3? Biochim. Biophys. Acta **1504**, 120–127

43   Brand, M. D., Pakay, J. L., Ocloo, A., Kokoszka, J., Wallace, D. C., Brookes, P. S. and Cornwall, E. J. (2005) The basal proton conductance of mitochondria depends on adenine nucleotide translocase content. Biochem. J. **392**, 353–362

44   Bauer, M. K., Schubert, A., Rocks, O. and Grimm, S. (1999) Adenine nucleotide translocase-1, a component of the permeability transition pore, can dominantly induce apoptosis. J. Cell Biol. **147**, 1493–1502

45   Vyssokikh, M. Y., Katz, A., Rueck, A., Wuensch, C., Dorner, A., Zorov, D. B. and Brdiczka, D. (2001) Adenine nucleotide translocator isoforms 1 and 2 are differently distributed in the mitochondrial inner membrane and have distinct affinities to cyclophilin D. Biochem. J. **358**, 349–358

46   Zamora, M., Merono, C., Vinas, O. and Mampel, T. (2004) Recruitment of NF-κB into mitochondria is involved in adenine nucleotide translocase 1 (ANT1)-induced apoptosis. J. Biol. Chem. **279**, 38415–38423

47   Chevrollier, A., Loiseau, D., Chabi, B., Renier, G., Douay, O., Malthiery, Y. and Stepien, G. (2005) ANT2 isoform required for cancer cell glycolysis. J. Bioenerg. Biomembr. **37**, 307–316

48   Dorner, A., Giessen, S., Gaub, R., Grosse Siestrup, H., Schwimmbeck, P. L., Hetzer, R., Poller, W. and Schultheiss, H. P. (2006) An isoform shift in the cardiac adenine nucleotide translocase expression alters the kinetic properties of the carrier in dilated cardiomyopathy. Eur. J. Heart Fail. **8**, 81–89

49   Brustovetsky, N. and Klingenberg, M. (1994) The reconstituted ADP/ATP carrier can mediate H$^+$ transport by free fatty acids, which is further stimulated by mersalyl. J. Biol. Chem. **269**, 27329–27336

50   Brustovetsky, N. N., Egorova, M. V., Gnutov, D., Gogvadze, V. G., Mokhova, E. N. and Skulachev, V. P. (1992) Thermoregulatory, carboxyatractylate-sensitive uncoupling in heart and skeletal muscle mitochondria of the ground squirrel correlates with the level of free fatty acids. FEBS Lett. **305**, 15–17